Histone Deacetylase AtHDA7 Is Required for Female Gametophyte and Embryo Development in Arabidopsis[1][C][W][OPEN]

Riccardo Aiese Cigliano[2], Gaetana Cremona, Rosa Paparo, Pasquale Termolino, Giorgio Perrella[3], Ruben Gutzat, Maria Federica Consiglio, and Clara Conicella*

National Research Council of Italy, Institute of Plant Genetics, Research Division Portici, 80055 Portici, Italy (R.A.C., G.C., R.P., P.T., G.P., M.F.C., C.C.); and Gregor Mendel Institute of Molecular Plant Biology, Austrian Academy of Sciences, 1030 Vienna, Austria (R.G.)

ORCID ID: 0000-0002-9678-0077 (C.C.)

Histone modifications are involved in the regulation of many processes in eukaryotic development. In this work, we provide evidence that *AtHDA7*, a *HISTONE DEACETYLASE* (*HDAC*) of the *Reduced Potassium Dependency3* (*RPD3*) superfamily, is crucial for female gametophyte development and embryogenesis in Arabidopsis (*Arabidopsis thaliana*). Silencing of *AtHDA7* causes degeneration of micropylar nuclei at the stage of four-nucleate embryo sac and delay in the progression of embryo development, thereby bringing the seed set down in the *Athda7-2* mutant. Furthermore, *AtHDA7* down- and up-regulation lead to a delay of growth in postgermination and later developmental stages. The *Athda7-2* mutation that induces histone hyperacetylation significantly increases the transcription of other *HDACs* (*AtHDA6* and *AtHDA9*). Moreover, silencing of *AtHDA7* affects the expression of *ARABIDOPSIS HOMOLOG OF SEPARASE* (*AtAESP*), previously demonstrated to be involved in female gametophyte and embryo development. However, chromatin immunoprecipitation analysis with acetylated H3 antibody provided evidence that the acetylation levels of H3 at *AtAESP* and *HDACs* does not change in the mutant. Further investigations are essential to ascertain the mechanism by which *AtHDA7* affects female gametophyte and embryo development.

DNA of eukaryotic cells is associated with nuclear proteins to form the chromatin. Its basic unit is the nucleosome, which is composed of about 147 bp of DNA bound to an octamer of the canonical histones H3, H4, H2A, and H2B (Berr et al., 2011). Histone posttranslational modifications contribute to define chromatin states that drive different chromatin-based nuclear processes. In fact, histone posttranslational modifications, including acetylation, methylation, phosphorylation, and ubiquitination, control fundamental processes such as transcription (Bell et al., 2011), DNA replication (Ehrenhofer-Murray, 2004), cell cycle (O'Sullivan et al., 2010), DNA repair (Soria et al., 2012), and recombination (Perrella et al., 2010). Histone acetylation is carried out by histone acetylases (HATs), while it is erased by histone deacetylases (HDACs). Plant HDACs are grouped into three families: the RDP3/HDA1 superfamily, SIR2, and HD2 (Pandey et al., 2002). Two of these families are homologous to the classes of HDACs found in yeast and animals, while the HD2 class appears to be unique to plants and unrelated to the other classes. In Arabidopsis (*Arabidopsis thaliana*), 18 putative HDACs have been identified (Pandey et al., 2002). Some HDACs are emerging as crucial players in plant growth and development processes, including embryogenesis, flowering, meiosis, senescence, as well as responses to environmental cues (Hollender and Liu, 2008; Berr et al., 2011). In particular, mutations in genes encoding HDACs as well as treatments with trichostatin A (TSA), an inhibitor of HDACs, highlighted a requirement of the HDACs in reproductive development. Indeed, the down-regulation of *AtHDA19* induced delayed flowering, flower abnormalities, embryonic defects, and seed set reduction (Tian et al., 2003). Silencing as well as overexpression of *AtHD2A* severely affected seed development (Wu et al., 2000; Zhou et al., 2004). The *Athda6* mutant was reported to exhibit reduced fertility to some extent (Aufsatz et al., 2002), and mutation of *AtHDA9* led to an early-flowering phenotype in short-day-grown plants (Kim et al., 2013). Some findings strongly suggest a role for *AtHDA7* in Arabidopsis reproduction. Indeed, *AtHDA7* (At5g35600), encoding a putative HDAC of the Reduced Potassium Dependency3 (RPD3) superfamily, is preferentially

[1] This work was supported by the European Union Seventh Framework Programme (grant no. KBBE–2009–222883).

[2] Present address: Sequentia Biotech SL, Bellaterra-Cerdanyola del Vallès, 08193 Barcelona, Spain.

[3] Present address: Plant Science Group, University of Glasgow, Glasgow G12 8QQ, UK.

* Address correspondence to conicell@unina.it.

The author responsible for distribution of materials integral to the findings presented in this article in accordance with the policy described in the Instructions for Authors (www.plantphysiol.org) is: Clara Conicella (conicell@unina.it).

[C] Some figures in this article are displayed in color online but in black and white in the print edition.

[W] The online version of this article contains Web-only data.

[OPEN] Articles can be viewed online without a subscription.

www.plantphysiol.org/cgi/doi/10.1104/pp.113.221713

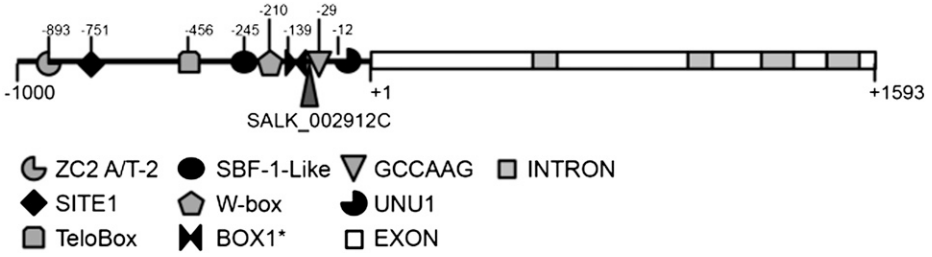

Figure 1. Schematic representation of the *AtHDA7* gene structure and its promoter region. The dark gray triangle indicates the position of the Transfer-DNA in Salk_002912C.

expressed in flower bud (Schmid et al., 2005) and is up-regulated in microdissected hyperacetylated microsporocytes (Barra et al., 2012). To investigate the unexplored function of *AtHDA7*, we analyzed overexpression and silenced mutants, thereby proving that *AtHDA7* is required for female gametophyte development and embryogenesis progression. Moreover, *AtHDA7* down- and up-regulation lead to a delay of growth in postgermination and later developmental stages.

RESULTS

In Silico Analysis of AtHDA7

AtHDA7 (At5g35600) encodes a putative histone deacetylase belonging to class I of the RPD3 superfamily characterized by a Histone_deacetylase domain (PF00850; Pandey et al., 2002). This superfamily includes the homologs of yeast RPD3 that preferentially deacetylate histones H3 and H4 (Rundlett et al., 1996). *AtHDA7* has five exons and four introns (www.arabidopsis.org) spanning 1,593 bp. To identify putative cis-regulatory motifs within the *AtHDA7* promoter, a region of 1,000 bp upstream of the translation start codon was analyzed in silico (Fig. 1). Eight motifs were identified between nucleotides −893 and −12. The motif at position −245 is similar to the binding site of SBF1, a transcriptional repressor (Lawton et al., 1991). On the other hand, motifs including ZC2 recognized by chromatin remodelers with zinc-finger domains (Ponte et al., 1994), telobox recognized by Athb homeodomain proteins (Sessa et al., 1993), W-box recognized by WRKY transcription factors (Eulgem et al., 2000), BOX1* (Tjaden et al., 1995), and GCCAAG motif (Leah et al., 1994) are reported to be involved in transcriptional activation. The predicted motif composition of the *AtHDA7* promoter suggests that its transcription is regulated in a complex way.

Overexpression and Silencing of *AtHDA7* Affect Growth

AtHDA7 was reported to be highly expressed in flower bud stage 9 (Schmid et al., 2005). In order to investigate *AtHDA7* function, the insertion line Salk_002912C (Alonso et al., 2003) was analyzed in this work. The Transfer-DNA insertion was confirmed to be in the putative promoter 43 bp upstream of the start codon, thereby introducing a gap between the GCCAAG activation motif and other motifs including SBF1-like (Fig. 1). Interestingly, *AtHDA7* was overexpressed in the mutant, with a change of 246-fold with respect to the wild type (Supplemental Fig. S1). Consequently, the mutant is herein designated *Athda7*^{oe}.

To silence *AtHDA7*, we generated transgenic plants constitutively expressing an artificial microRNA. One heterozygous transgenic plant, showing a strong down-regulation of *AtHDA7* (*Athda7-2*; Fig. 2A), was selected for further characterization. To ascertain whether alteration of *AtHDA7* expression affected histone acetylation, immunoblotting with histone extracts from *Athda7-2* and the wild type was performed using an antibody specific for H3 diacetylated at Lys-9 and Lys-14. *Athda7-2* showed increased levels of H3 acetylation compared with the wild type ($P < 0.05$; Fig. 2B).

Seed germination and growth rate studies were carried out on *Athda7*^{oe} and *Athda7-2*. While seed germination rate was not affected in *Athda7*^{oe}, a significant reduction was exhibited by *Athda7-2* as compared with the wild type (89% versus 99%; $P < 0.001$; Fig. 3). Interestingly, a significant retardation of growth rate, measured as the number of vegetative leaves produced over time, was observed in vitro and in soil for *Athda7*^{oe} as well as *Athda7-2* (Figs. 4 and 5). For instance, 8 d after transfer of the imbibed seeds to growing conditions, 62% of *Athda7*^{oe} and 66% of *Athda7-2* seedlings reached growth stage 1.04, corresponding to four rosette leaves (Boyes et al., 2001), as compared with 94% of the wild type (Fig. 4). In *Athda7*^{oe} plants grown in soil, growth rate was significantly different from the wild type

Figure 2. Expression analysis of *AtHDA7* and the level of acetylated H3 in *Athda7-2* leaf. A, Quantitative RT-PCR. The fold change values are averages of three replicates. The SE is reported as a black vertical bar. B, Immunoblotting performed by anti-H3K9K14Ac and anti-H3 antibodies. The relative ratio of H3K9K14Ac/H3 and SE (three replicates) are reported in the bar diagram. *$P < 0.05$. WT, Wild type.

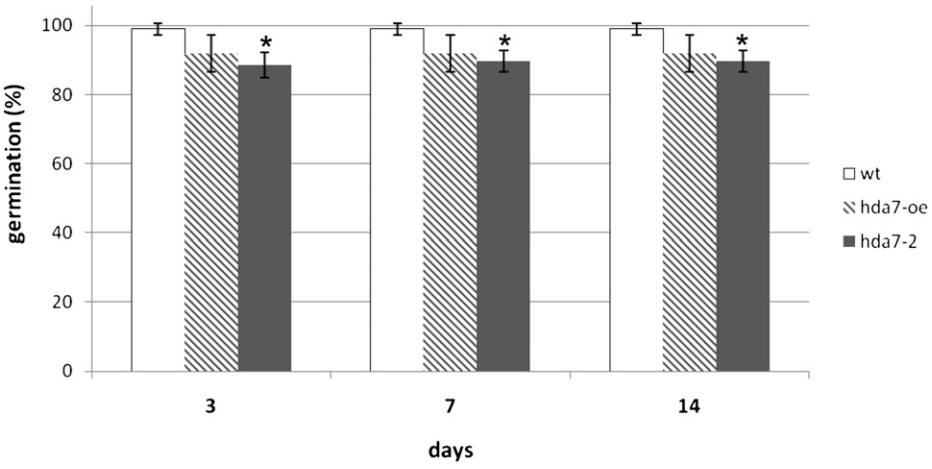

Figure 3. Seed germination in *Athda7*^{oe} (n = 124) and *Athda7-2* (n = 316) as compared with the wild type (wt; n = 125). Radicle emergence (stage 0.5 according to Boyes et al., 2001) or later stages were recorded at reported days relative to the date of seed incubation at 24°C. Seeds were preincubated at 4°C for 4 d. Average values are shown with SD. *$P \leq 0.001$.

starting on day 11 after sowing, while *Athda7-2* plants diverged significantly from the wild type 25 d after sowing (Fig. 5). Furthermore, flowering time, measured as the number of leaves at bolting, was significantly different ($P < 0.05$) between the wild type (11.2 ± 1.1 leaves) and *Athda7*^{oe} (9 ± 0.9 leaves) but was not affected in *Athda7-2* (9.6 ± 1.3 leaves). Collectively, these findings highlight that both up- and down-regulation of *AtHDA7* lead to a delay of growth.

Down-Regulation of *AtHDA7* Affects Fertility

Pollen viability in *Athda7*^{oe} and *Athda7-2* did not differ from that in the wild type. Silique fertility in *Athda7*^{oe} was similar to the wild type, whereas the number of fully developed seeds per silique decreased in *Athda7-2* due to unfertilized ovules and aborted seeds (Fig. 6). Accordingly, the length of mature siliques was significantly reduced by 14% in *Athda7-2* (1.2 ± 0.1 cm) with respect to the wild type (1.4 ± 0.1 cm). In order to evaluate whether AtHDA7 is required for the development of the female gametophyte, we assessed the transmission efficiency of the mutated allele linked to the *nptII* gene, the selectable marker used to obtain *Athda7-2*. The progeny of reciprocal crosses between heterozygous *Athda7-2* and the wild type were scored in vitro for kanamycin resistance and confirmed by genotyping. As shown in Table I, 50% of the progeny were resistant to kanamycin when the mutant was used as male, thereby indicating that transmission efficiency was 100%, as expected. When the progeny of the reciprocal cross were analyzed, we found that only 33% were

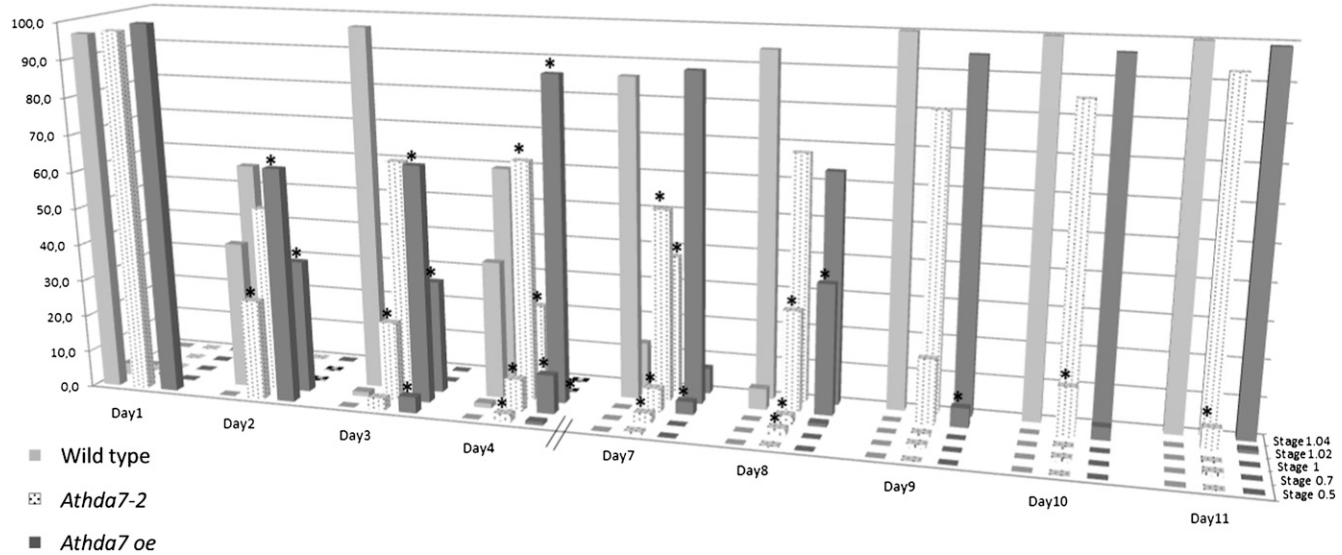

Figure 4. In vitro growth stages of seedlings in *Athda7*^{oe} (n = 114) and *Athda7-2* (n = 277) compared with the wild type (n = 120). The frequency of seedlings at stages from 0.5 to 1.04 (according to Boyes et al., 2001) was recorded at reported days relative to the date of seed incubation at 24°C. Seeds were preincubated at 4°C for 4 d. The values are averages of three replicates. *$P \leq 0.05$.

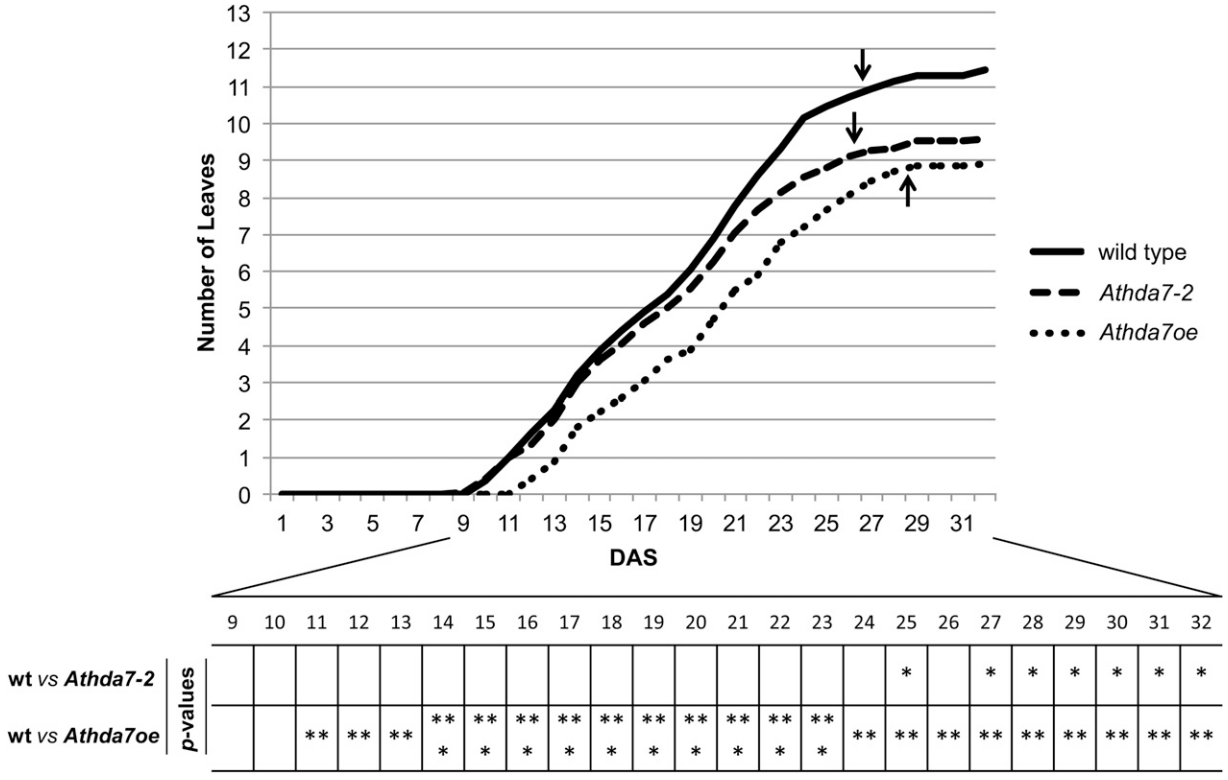

Figure 5. In soil growth of *Athda7*^{oe} ($n = 37$) and *Athda7-2* ($n = 40$) compared with the wild type (wt; $n = 35$). The number of rosette leaves was recorded over a period of 32 d after sowing (DAS). Flowering time is indicated by arrows. $^{*}P \leq 0.05$, $^{**}P \leq 0.01$, $^{***}P \leq 0.001$.

kanamycin resistant, showing a severe reduction in transmission efficiency to 51% of the expected 100% through the female gamete (Table I).

These findings highlight that *AtHDA7* down-regulation leads to partial failure of ovule/female gametophyte development and seed abortion.

AtHDA7 Is Required for Female Gametophyte and Embryo Development

The above-described phenotype suggests that ovule/female gametophyte development and seed/embryo development are impaired in the *Athda7-2* mutant. Megasporogenesis and megagametogenesis were observed in *Athda7-2* and the wild type by differential interference contrast (DIC) visualization of clarified carpels with length from 1 to 2 mm to identify the developmental stages affected by the *Athda7-2* mutation. In wild-type Arabidopsis, one megaspore mother cell per ovule undergoes meiosis and a tetrad of megaspores is produced. Subsequently, one surviving functional megaspore at the chalazal position undergoes gametogenesis. The production of functional megaspores observed in *Athda7-2* (Supplemental Fig. S2) indicates that

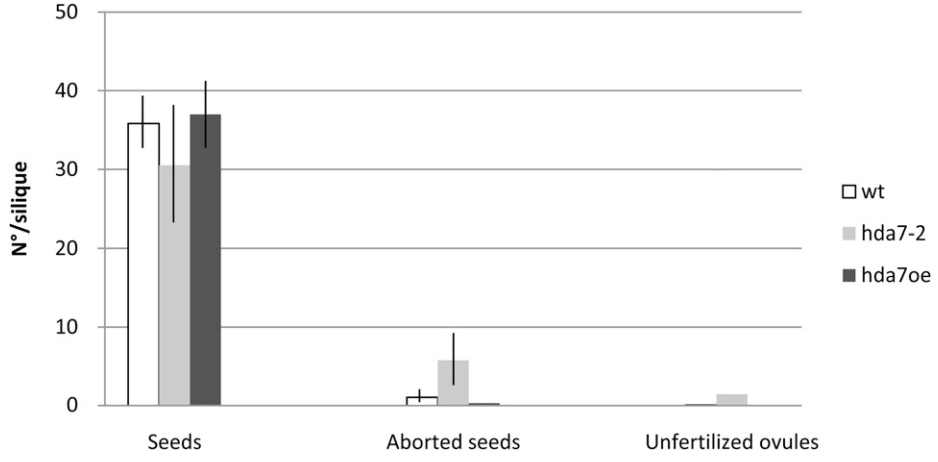

Figure 6. Silique fertility in *Athda7*^{oe} and *Athda7-2* compared with the wild type (wt). Average values estimated on 20 siliques are shown with SD.

Table I. *Transmission efficiency of the Athda7-2 allele estimated in reciprocal crosses between the heterozygous mutant (AtHDA7/Athda7-2) and the wild type (AtHDA7/AtHDA7)*

Sample	Total Seeds	*nptII*$^+$	*nptII*$^-$	Transmission Efficiency[a]	
				Observed	Expected
		n			
Reciprocal crosses					
AtHDA7/Athda7-2 × *AtHDA7/AtHDA7*	62	21	41	51	100
AtHDA7/AtHDA7 × *AtHDA7/Athda7-2*	40	20	20	100	100
Selfings					
AtHDA7/Athda7-2 × *AtHDA7/Athda7-2*	50	25	25	–	–
AtHDA7/AtHDA7 × *AtHDA7/AtHDA7*	50	0	50	–	–

[a]Transmission efficiency = (number of *nptII*$^+$ seedlings/number of *nptII*$^-$ seedlings) × 100 through female or male gametes according to Brukhin et al. (2011).

female meiosis is apparently regular in *Athda7-2*. However, in *Athda7-2* carpels of 1.3 mm, which contained mostly ovules with two/four-nucleate embryo sacs (ES), 12% of ovules (n = 40) still harbor megaspore mother cells undergoing meiosis, thereby suggesting a delayed progression of female meiosis (Supplemental Fig. S3).

In wild-type Arabidopsis, the functional megaspore undergoes three rounds of mitosis, producing an eight-nucleate/seven-celled ES (Fig. 7, A–F). In *Athda7-2* (Fig. 7, G–L), defects were observed during the progression of megagametogenesis, followed according to the stages described by Christensen et al. (1997). While no deviation was observed in female gametophyte (FG) stages FG2 to FG3 (corresponding to two-nucleate ES; Fig. 7H), at stage FG4 of four-nucleate ES, 10% of *Athda7-2* ovules (n = 80) showed ES with the pair of micropylar nuclei in degeneration (Fig. 7J; Supplemental Fig. S3). In FG5 to FG6, *Athda7-2* carpels of 1.7 and 2.0 mm showed both ovules with regular ES (Fig. 7K) and ovules with the first degeneration signs (Supplemental Figs. S3 and S4). Mature *Athda7-2* ES undergoing a normal fate exhibited nuclear migration and cellularization. 4′6-Diamidino-2 phenylindole (DAPI) staining of *Athda7-2* ovules (n = 128) excised from pistils at the prefertilization stage revealed that 14% of the ES were collapsed (Fig. 7L), confirming the findings of DIC visualization. Ovules in degeneration were also observed in pistils after fertilization (Fig. 8B). Based on the cytological findings, AtHDA7 is required for ES development.

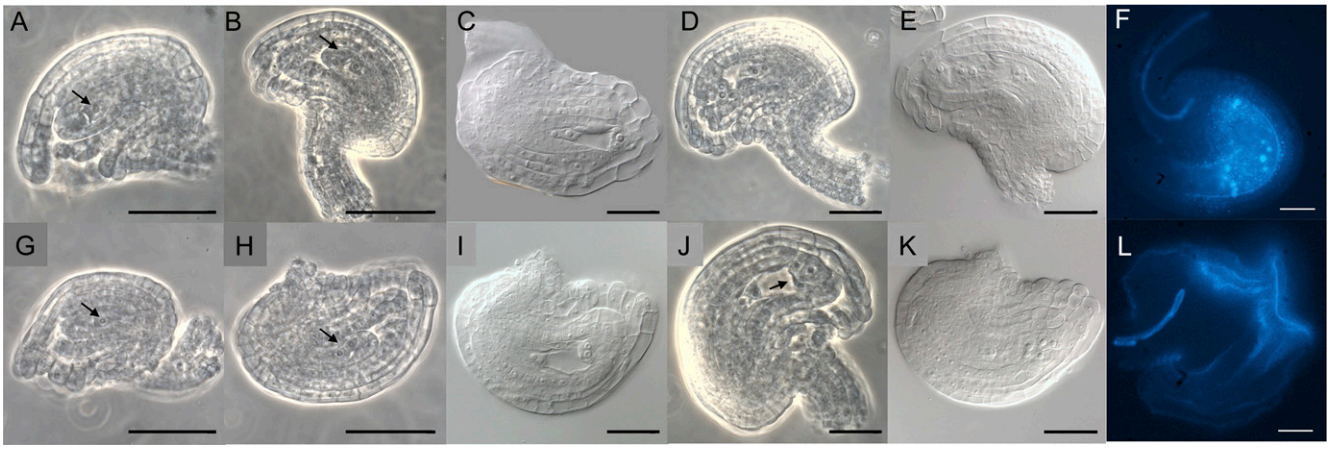

Figure 7. Ovule and female gametophyte development in the wild type (A–F) and *Athda7-2* (G–L). A and G, One-nucleate female gametophyte at stage FG1 (according to Christensen et al., 1997), indicated by the arrows. Degenerate megaspores are present. B and H, Two-nucleate female gametophyte at stage FG2, indicated by the arrows. C, D, and I, Four-nucleate female gametophyte at late stage FG4. Two pairs of nuclei at each pole are separated by a large central vacuole, and the chalazal nuclei are positioned along a line that is parallel to the chalazal-micropylar axis. J, Female gametophyte at late stage FG4 showing micropylar nuclei in degeneration, indicated by the arrow. E and K, Eight-nucleate/seven-celled mature female gametophyte. Observations were performed by DIC (C, E, I, and K) and phase-contrast microscopy. The female gametophyte in A, B, D, E, and G is oriented with its micropylar pole to the left, while the micropylar pole in C, H, I, J, and K is at right. F and L, Ovules excised from prefertilization pistils and observed by fluorescence microscopy through DAPI staining. In *Athda7-2*, the ovule is degenerating. Bars = 20 μm. [See online article for color version of this figure.]

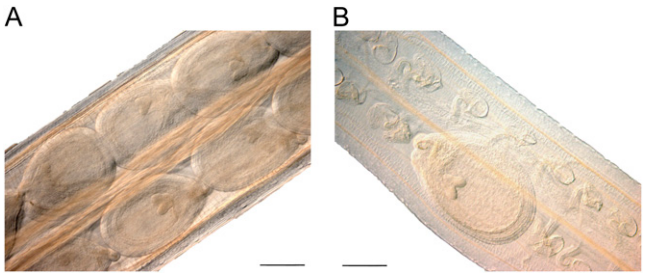

Figure 8. Embryogenesis in the wild type (A) and *Athda7-2* (B). A, All embryos are at the heart stage. B, One embryo is at the heart stage, while the remaining ovules are degenerating. Bars = 200 μm. [See online article for color version of this figure.]

In order to identify the cause of seed abortion, *Athda7-2* clarified pistils after fertilization were analyzed by DIC microscopy (Fig. 8). Embryonic stages observed within the silique were strongly asynchronous in *Athda7-2*, suggesting a delay in the progression of embryo development. At 10 d after pollination, only 67% of *Athda7-2* embryos (n = 686) had reached linear or torpedo stages compared with 90% of wild-type embryos (Fig. 9; $P < 0.001$). The remaining 33% of *Athda7-2* embryos were at heart or earlier stages.

The above-reported findings indicate that AtHDA7 is required for both female gametophyte and embryo development.

Other *HDACs* and *AtAESP* Are Misregulated in *Athda7-2*

In order to verify whether a misregulation occurred in RPD3 HDAC members, quantitative reverse transcription (RT)-PCR analysis was performed to monitor the expression of *AtHDA6*, *AtHDA9*, and *AtHDA19* in *Athda7-2*. As shown in Figure 10A, *AtHDA6* and *AtHDA9* levels were significantly up-regulated in *Athda7-2*. On the contrary, *AtHDA19* was down-regulated, with a change of 0.8-fold ($P < 0.005$). To test the possibility that the higher expression of *AtHDA6* and *AtHDA9* in *Athda7-2* originate from a distinct chromatin configuration at these loci, a chromatin immunoprecipitation (ChIP) analysis with anti-acetyl-histone H3 antibody was performed. As shown in Supplemental Figure S5, neither *AtHDA6* nor *AtHDA9* displayed hyperacetylation of histone H3 in *Athda7-2* compared with the wild-type.

To find additional genes misregulated in the *Athda7-2* background, the Expression Angler tool (http://bar.utoronto.ca/ntools) was used to identify genes coregulated with *AtHDA7* at developmental stages corresponding to gametogenesis. This analysis showed that 589 and 317 genes were positively coregulated with *AtHDA7* in embryos and flower buds, respectively, whereas no negatively coregulated genes were identified. In embryos, the majority of *AtHDA7* coregulated genes related to protein metabolism, response to stress, and developmental processes (Supplemental Fig. S6A; Supplemental Table S1), while in flowers and ovaries, coregulated genes were classified as involved in protein metabolism, developmental processes, cell organization, and biogenesis (Supplemental Fig. S6B; Supplemental Table S1). For experimental validation, *ARABIDOPSIS HOMOLOG OF SEPARASE* (*AtAESP*) was selected, given its role in ovule and embryo development (Liu and Makaroff, 2006; Yang et al., 2011). As shown in Figure 10B, *AtAESP* was significantly down-regulated in *Athda7-2* flower buds, with a change of 0.64-fold ($P < 0.002$) compared with the wild type. We examined whether *AtHDA7* down-regulation affected the histone acetylation status of *AtAESP* by ChIP analysis with anti-acetyl-histone H3 antibody. *AtAESP* did not demonstrate any acetylation variation of histone H3 in *Athda7-2* compared with the wild type (Supplemental Fig. S5).

DISCUSSION

In this work, the functional analysis of *AtHDA7* was performed by means of mutations inducing overexpression in *Athda7*^{oe} and silencing and histone hyperacetylation in

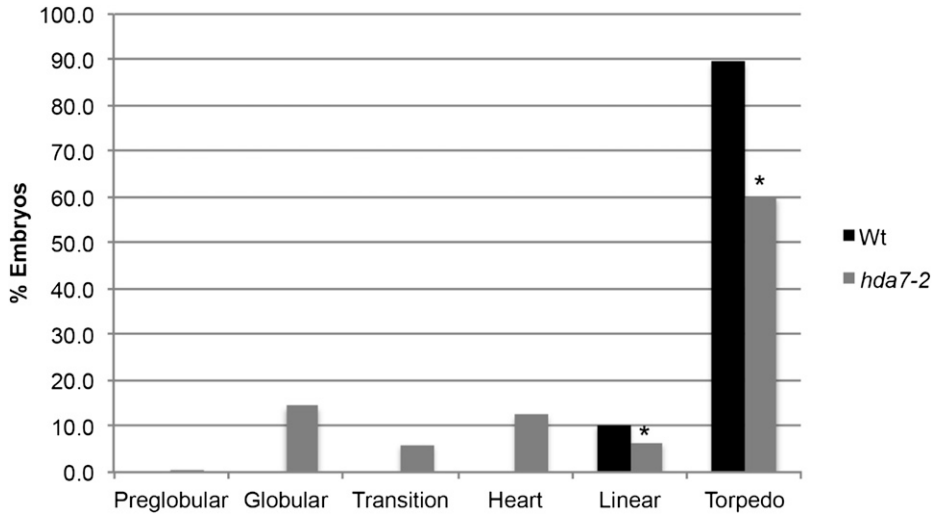

Figure 9. Embryo stages in the wild type (Wt) and *Athda7-2* at 10 d after pollination. *$P < 0.05$.

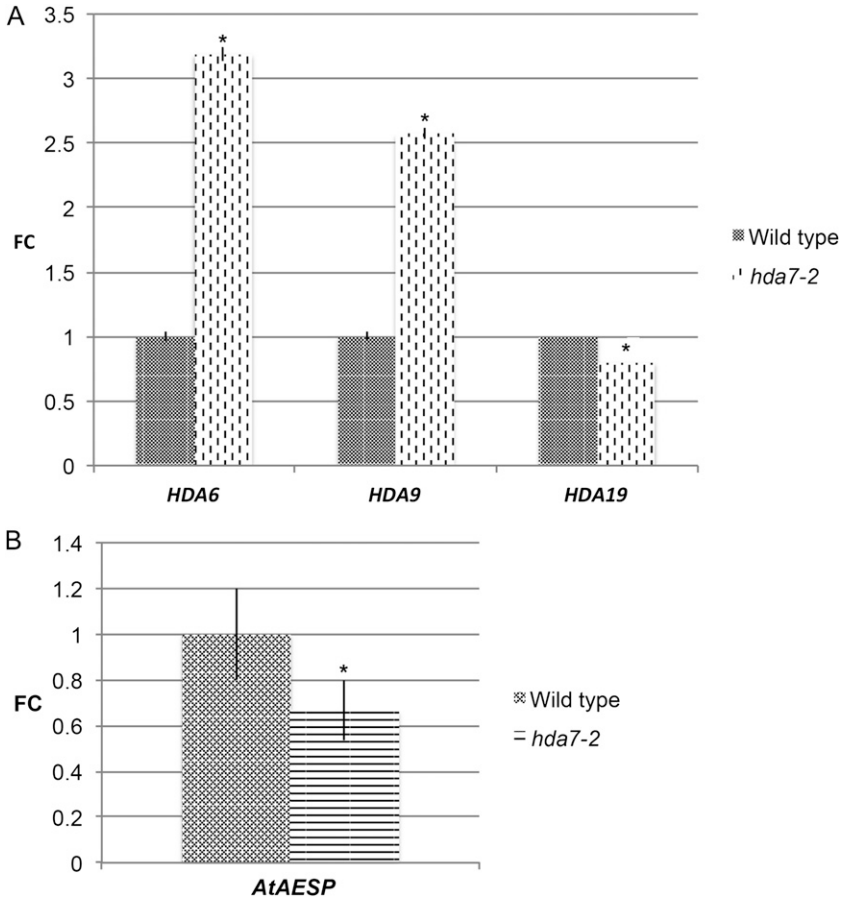

Figure 10. Expression analysis of *AtHDA6*, *AtHDA9*, and *AtHDA19* in *Athda7-2* leaf (A) and of *AtAESP* in flower bud (B) in comparison with the wild type. The fold change (FC) values are averages of three replicates. The SE is reported as a black vertical bar. $*P < 0.05$.

Athda7-2. Both down- and up-regulation of *AtHDA7* caused delays of growth at different developmental stages. An analogous phenomenon was reported in *AtHDA18*, with a similar altered cellular patterning in the root epidermis of overexpressing and knockdown mutants (Liu et al., 2013). The decreased seed germination phenotype of *Athda7-2* demonstrates the importance of histone deacetylation in early development. The reduction of germination rates was observed in seeds treated with TSA (Tanaka et al., 2008). However, seed germination was unaffected in *Athda6* as well as in the double *Athda6/Athda19* mutant (Tanaka et al., 2008; Chen et al., 2010). In *Athd2a* and *Athd2c* mutants, Colville and colleagues (2011) reported defects in seed germination due to altered responses to sugar. They found that *AtHD2A* prevents germination while *AtHD2C* enhances germination in the presence of Glc. In contrast to *AtHD2A* and *AtHD2C*, *AtHDA7* is not induced by Glc (Colville et al., 2011), thereby making it unlikely that sugar sensing is involved in the seed germination defects observed in *Athda7-2*. The similarity between the *Athda7-2* phenotype and TSA treatment (Tanaka et al., 2008) suggests a role for *AtHDA7* in Arabidopsis seed germination. With regard to the defects in postgermination growth observed in *Athda7-2*, similar behavior was exhibited by the *Athda6/Athda19* double mutant and TSA-treated seeds (Tanaka et al., 2008). *AtHDA7* seems to be not required by itself for Arabidopsis growth, which, instead, is controlled by the concerted action of different HDACs in response to the environment.

Female gametophyte and embryo development were affected in *Athda7-2* mutants, while *Athda7*^{oe} lacked unfertilized ovules and aborted seeds, indicating normal ES and embryo development. In the silenced mutant, homozygous individuals for *nptII* gene coding for kanamycin resistance were not recovered in the selfings of *Athda7-2*. A likely explanation is that a portion of the female gametophytes carrying the silenced allele and the embryos with both silenced alleles abort during their respective development. The gametophytic mutation is partially penetrant, as observed by the reduced transmission of the silenced allele through the female gametophyte and by microscopic analysis indicating 10% defective *Athda7-2* ES at the four-nucleate stage. Micropylar nuclei were seen to degenerate, and ovules harboring nonfunctional female gametophytes failed to undergo seed development. Several studies have highlighted the importance of nuclei migration and positioning for female gametophyte development (Sprunck and Gross-Hardt, 2011). At the late four-nucleate stage, the pair of sister nuclei at both poles of the ES acquire the position, along the micropylar-chalazal axis (long axis), that critically determines their fate. In particular, micropylar nuclei are fated to become the egg apparatus. *AtHDA7* is required specifically for female (not for male)

gametophyte development in Arabidopsis, particularly at the four-nucleate stage. Only HAM1 and HAM2, belonging to MYST HATs, were described as essential for female as well as male gametophyte development in Arabidopsis (Latrasse et al., 2008). In *HAM1/ham1; ham2/ham2* and *ham1/ham1; HAM2/ham2* plants, half of the ovules aborted, since megagametogenesis failed to progress beyond the one-nucleate stage.

Besides ES collapse before fertilization, seed failures in *Athda7-2* are likely due to a noticeable delay in embryogenesis progression. This indicates that *AtHDA7* is required for embryogenesis. Studies concerning the relationships between histone deacetylation/acetylation and embryogenesis have been reported in Arabidopsis (Long et al., 2006) as well as in maize (*Zea mays*), where HATs and HDACs were first isolated in embryos (Kölle et al., 1999). Varotto and colleagues (2003) showed that ZmHDA108, the closest homolog to *AtHDA7*, is particularly abundant in kernels at 3 to 8 d after pollination and in embryos. Although *ZmHDA108* was not functionally analyzed, its expression profile suggests a role in embryo development.

Since HDACs are transcriptional regulators, we identified the genes coregulated with *AtHDA7* by an in silico approach. Among these genes, the separase *AtAESP* that was down-regulated in *Athda7-2* may provide some insight into the role of *AtHDA7*. *AtAESP* is required for ovule and embryo development in Arabidopsis (Liu and Makaroff, 2006; Yang et al., 2011). Loss of separase activity dramatically slows the progression of megagametogenesis and embryogenesis. It was speculated that separase could prevent cyclin destruction, as demonstrated in yeast (Tinker-Kulberg and Morgan, 1999). It might be hypothesized that *AtHDA7* interacts with histones associated with *AtAESP*. However, based on ChIP-PCR analysis performed in this work, the histone acetylation level in the *AtAESP* locus does not change in *Athda7-2*.

In the silenced mutant, a relationship exists between the expression of AtHDA7 and the other HDACs, including *AtHDA6*, *AtHDA9*, and *AtHDA19*. The lack of enhancement of H3 acetylation at *AtHDA6* and *AtHDA9* loci rules out that these genes are direct targets of AtHDA7, suggesting that other factors are involved in their transcription regulation. HDAC misregulation could be triggered by a compensatory effect for histone deacetylation to remedy the down-regulation of *AtHDA7*. It has been reported that the expression of HATs/HDACs is affected in Arabidopsis and maize upon changes in the degree of acetylation (Bhat et al., 2003; Tian et al., 2005). In particular, in the HAT mutant *Atmcc1*, characterized by histone hyperacetylation in meiosis, *AtHDA7* resulted in up-regulated male meiocytes (Perrella et al., 2010; Barra et al., 2012). The misregulation of the different HDACs in *Athda7-2* likely affects the expression of different classes of genes. For example, *AtHDA19* is down-regulated in *Athda7-2* and is considered to be a global regulator of gene expression in Arabidopsis, controlling 11% and 8% of the transcriptome in leaf and flower, respectively (Tian et al., 2005). *AtHDA19* as well as *AtHDA6* and *AtHDA9* are involved in several aspects of plant development (Aufsatz et al., 2002; Earley et al., 2006; Fong et al., 2006; Kim et al., 2013).

The findings reported in this study provide evidence that AtHDA7 is required for female gametophyte and embryo development as well as plant growth in Arabidopsis. However, further investigation is essential for elucidating the underlying mechanisms.

MATERIALS AND METHODS

Plant Materials and Phenotype Analyses

Arabidopsis (*Arabidopsis thaliana*) material includes Salk_002912C (herein *hda7*^{oe}), amiHDA7 lines (herein *Athda7-1* and *Athda7-2*), and Columbia as the wild type. Plants were grown in controlled conditions with 16 h/8 h of light/dark at 22°C/18°C. In vitro culture was performed as described by Weigel and Glazebrook (2002). For transformation, *Agrobacterium tumefaciens* GV3101 and the floral spray method were used (Chung et al., 2000). Transformants were selected on kanamycin (50 mg L^{-1}). Seed germination was scored at 3, 7, and 14 d after 4-d stratification as described by Tanaka and colleagues (2008). The growth rate of seedlings (stages 0.5–1.04) was estimated according to Boyes et al. (2001). Soil-based analysis of growth was performed every 2 d by counting the number of rosette leaves more than 1 mm in length produced over 31 d according to Boyes et al. (2001).

In Silico Analysis of HDA7

The gene structure of *HDA7* (At5g35600) was obtained from The Arabidopsis Information Resource (http://www.arabidopsis.org). An area 1,000 bp upstream of the predicted start codon of *HDA7* was analyzed with NSITE-PL (http://linux1.softberry.com) and Akiyama's TFSEARCHv1.3 (http://molsun1.cbrc.aist.go.jp/research/db/TFSEARCH.html) with default setting to detect putative regulatory motifs.

Artificial MicroRNA

The specific artificial microRNA to silence *AtHDA7* (amiHDA7) and the oligonucleotide sequences were designed using the WMD3 Web tool according to the procedures and criteria described by Schwab and colleagues (2010; http://wmd3.weigelworld.org/cgi-bin/webapp.cgi). The predicted mature microRNA sequence was 5′-UUAGACAAGUUGAAUGUGCCA-3′. Primers used in the construction of amiHDA7 are listed in Supplemental Table S2. The cloning of amiHDA7 was performed using the miR319a precursor-containing plasmid pRS300 as a template (Schwab et al., 2010). Primers A and B were modified to allow the cloning of the final PCR product with Gateway technology into pK2GW7 binary vector (http://gateway.psb.ugent.be) using pDONR/ZEO (Invitrogen) as donor. Eleven transgenic lines with a single insertion were obtained (Supplemental Table S3).

Expression Analysis

Total RNA was extracted from young leaves and floral buds using the RNeasy Plant Mini Kit (Qiagen) and treated with DNase I (Invitrogen). To obtain complementary DNA, SuperScript III Two-Step RT-PCR and Oligo$(dT)_{12\text{-}18}$ (Invitrogen) were used following the manufacturer's instructions. Gene-specific primers designed using Primer Express software, version 2.0 (Applied Biosystems), are listed in Supplemental Table S4. Real-time RT-PCR was carried out using Rotor-Gene 6000 (Corbett) with FastStart SYBR Green Master (Roche). The *ADENOSINE PHOSPHORIBOSYL TRANSFERASE1* gene was used as reference.

ChIP

For ChIP analysis, 3-week-old seedlings were used. For immunoprecipitation, antibodies against acetylated histone H3 (Millipore; catalog no. 06-599), histone H3 (Abcam; catalog no. 1791), and unspecific IgG (from rabbit; Diagenode) were used. Cross linking and immunoprecipitation were performed with the LowCell Number ChIP kit from Diagenode as described previously

(Gutzat et al., 2011). DNA was analyzed by quantitative PCR on a Roche Light Cycler 96 instrument and with the FastStart SYBR Green Master mix (Roche) according to the manufacturer's instructions. For quantification, results from two PCRs were used. All ChIP experiments were performed with two biological replicates. Primer sequences were chosen either in highly histone H3-acetylated regions at the 5′ end of the open reading frame of *AtHDA6* (At5g63119), *AtHDA9* (At3g44680), or *AtAESP* (At4g22970) or farther downstream in less acetylated regions. Primer sequences are listed in Supplemental Table S5.

Immunoblotting

Histone-enriched protein extracts were prepared according to Gendrel et al. (2002). The chromatin was treated twice with 0.4 M sulfuric acid, and the proteins were precipitated with 20% TCA. All the buffers were supplemented with 0.1 mM phenylmethylsulfonyl fluoride and proteinase inhibitor tablets (Complete Mini; Roche). For hybridization, H3K9K14Ac antibody (Diagenode; pAb-005-044) was incubated overnight in a 1:1,000 dilution in 1% milk Tris-buffered saline plus Tween 20 buffer. To normalize histone levels, membrane was reprobed with H3 antibody (Abcam; Ab1791). Immunoblotting was replicated three times. The hybridizing bands were quantified using ImageJ software.

Analysis of Fertility-Associated Traits

Pollen viability was assessed by Alexander's staining (Alexander, 1969). For megagametophyte analysis, ovules were excised from different-sized pistils (1, 1.3, 1.5, 1.7, and 2 mm) previously fixed in ethanol:acetic acid (3:1, v/v). They were cleared with a chloral hydrate solution (8 g of chloral hydrate, 1 mL of glycerol, and 2 mL of water) and examined with the Leica DM6000B microscope equipped with DIC and phase-contrast optics. In addition, ovules dissected from pistils in floral buds at stage 13 (Smyth et al., 1990), clarified in 85% solution of lactic acid and phenol (2:1, w/w) for 30 min, and stained with 10 μg mL^{-1} DAPI were observed with a Leica DMR microscope equipped with fluorescence. For embryo development analysis, seeds within siliques were examined by DIC microscopy according to Meinke et al. (1994). Finally, the length of mature siliques, the seed set, and the unfertilized ovules were assessed at stages 17 and 18 (Smyth et al., 1990) by stereomicroscopy at a magnification of 20×.

Statistical Analyses

A χ^2 test was used in the segregation analysis and in the growth rate experiments. Student's *t* test was used in real-time RT-PCR analysis.

Analysis of Gene Coregulation

The Expression Angler tool (http://bar.utoronto.ca) was used to identify genes coregulated with *AtHDA7* during embryo and flower development. The expression data of the experiments selected for our analysis are listed in Supplemental Table S6. An *r* value cutoff ranging from 0.75 to 1.0 and from −0.75 to −1.0 was chosen.

Supplemental Data

The following materials are available in the online version of this article.

Supplemental Figure S1. Expression analysis of *AtHDA7* in *Athda7*^{oe} leaf with respect to the wild type.

Supplemental Figure S2. Ovule and megasporogenesis in *Athda7-2*: megaspore mother cell (A) and functional megaspore with degenerate megaspores (B).

Supplemental Figure S3. Stages (FG) of female gametophyte (ES) development in *Athda7-2* compared with the wild type according to Christensen et al. (1997).

Supplemental Figure S4. Degenerating ovules excised from pistils of 2 mm in *Athda7-2* observed by phase contrast.

Supplemental Figure S5. ChIP analysis of acetylation levels of histone H3 at *AtHDA6*, *AtHDA9*, and *AtAESP* in 3-week-old wild-type and *Athda7-2* seedlings.

Supplemental Figure S6. Functional annotation of *AtHDA7* coregulated genes in embryos (from globular to torpedo stage) and in ovaries and flowers (from stage 9 to stage 15; Smyth et al., 1990).

Supplemental Table S1. List of genes that are coregulated with *AtHDA7* in embryos (from globular to torpedo stage) and in ovaries and flowers (from stage 9 to stage 15; Smyth et al., 1990).

Supplemental Table S2. Primers used to clone amiHDA7.

Supplemental Table S3. Segregation analysis of T2 amiRNAi-HDA7 lines on selective media.

Supplemental Table S4. Primers used for real-time RT-PCR experiments.

Supplemental Table S5. Primers used for ChIP-PCR experiments.

Supplemental Table S6. List of the microarray experiments selected to identify AtHDA7 coregulated genes during embryo and flower development.

ACKNOWLEDGMENTS

We thank Giorgia Batelli (CNR, Institute of Plant Genetics), and Domenico Carputo and Michael J. Van Oosten (University of Naples Federico II) for critical reading of the manuscript. We thank Rosarita Tatè and Salvatore Arbucci of the Institute of Genetics and Biophysics Integrated Microscopy Facility for helping in DIC analysis. Assistance to ensure plant growth in controlled conditions was provided by Rosario Nocerino (CNR, Institute of Plant Genetics).

Received May 22, 2013; accepted July 21, 2013; published July 22, 2013.

LITERATURE CITED

Alexander MP (1969) Differential staining of aborted and nonaborted pollen. Stain Technol **44:** 117–122

Alonso JM, Stepanova AN, Leisse TJ, Kim CJ, Chen H, Shinn P, Stevenson DK, Zimmerman J, Barajas P, Cheuk R, et al (2003) Genome-wide insertional mutagenesis of Arabidopsis thaliana. Science **301:** 653–657

Aufsatz W, Mette MF, van der Winden J, Matzke M, Matzke AJM (2002) HDA6, a putative histone deacetylase needed to enhance DNA methylation induced by double-stranded RNA. EMBO J **21:** 6832–6841

Barra L, Aiese-Cigliano R, Cremona G, De Luca P, Zoppoli P, Bressan RA, Consiglio MF, Conicella C (2012) Transcription profiling of laser microdissected microsporocytes in an Arabidopsis mutant (atmcc1) with enhanced histone acetylation. J Plant Biol **55:** 281–289

Bell O, Tiwari VK, Thomä NH, Schübeler D (2011) Determinants and dynamics of genome accessibility. Nat Rev Genet **12:** 554–564

Berr A, Shafiq S, Shen WH (2011) Histone modifications in transcriptional activation during plant development. Biochim Biophys Acta **1809:** 567–576

Bhat RA, Riehl M, Santandrea G, Velasco R, Slocombe S, Donn G, Steinbiss HH, Thompson RD, Becker HA (2003) Alteration of GCN5 levels in maize reveals dynamic responses to manipulating histone acetylation. Plant J **33:** 455–469

Boyes DC, Zayed AM, Ascenzi R, McCaskill AJ, Hoffman NE, Davis KR, Görlach J (2001) Growth stage-based phenotypic analysis of *Arabidopsis*: a model for high throughput functional genomics in plants. Plant Cell **13:** 1499–1510

Brukhin VB, Jaciubek M, Bolaños Carpio A, Kuzmina V, Grossniklaus U (2011) Female gametophytic mutants of Arabidopsis thaliana identified in a gene trap insertional mutagenesis screen. Int J Dev Biol **55:** 73–84

Chen L-T, Luo M, Wang Y-Y, Wu K (2010) Involvement of Arabidopsis histone deacetylase HDA6 in ABA and salt stress response. J Exp Bot **61:** 3345–3353

Christensen CA, King EJ, Jordan JR, Drews GN (1997) Megagametogenesis in Arabidopsis wild type and the Gf mutant. Sex Plant Reprod **10:** 49–64

Chung MH, Chen MK, Pan SM (2000) Floral spray transformation can efficiently generate Arabidopsis transgenic plants. Transgenic Res **9:** 471–476

Colville A, Alhattab R, Hu M, Labbé H, Xing T, Miki B (2011) Role of HD2 genes in seed germination and early seedling growth in Arabidopsis. Plant Cell Rep **30:** 1969–1979

Earley K, Lawrence RJ, Pontes O, Reuther R, Enciso AJ, Silva M, Neves N, Gross M, Viegas W, Pikaard CS (2006) Erasure of histone acetylation by Arabidopsis HDA6 mediates large-scale gene silencing in nucleolar dominance. Genes Dev **20:** 1283–1293

Ehrenhofer-Murray AE (2004) Chromatin dynamics at DNA replication, transcription and repair. Eur J Biochem **271:** 2335–2349

Eulgem T, Rushton PJ, Robatzek S, Somssich IE (2000) The WRKY superfamily of plant transcription factors. Trends Plant Sci **5:** 199–206

Fong PM, Tian L, Chen ZJ (2006) Arabidopsis thaliana histone deacetylase 1 (AtHD1) is localized in euchromatic regions and demonstrates histone deacetylase activity in vitro. Cell Res **16:** 479–488

Gendrel AV, Lippman Z, Yordan C, Colot V, Martienssen RA (2002) Dependence of heterochromatic histone H3 methylation patterns on the Arabidopsis gene DDM1. Science **297:** 1871–1873

Gutzat R, Borghi L, Fütterer J, Bischof S, Laizet Y, Hennig L, Feil R, Lunn J, Gruissem W (2011) RETINOBLASTOMA-RELATED PROTEIN controls the transition to autotrophic plant development. Development **138:** 2977–2986

Hollender C, Liu Z (2008) Histone deacetylase gene in *Arabidopsis*. Dev J Integr Plant Biol **50:** 875–885

Kim W, Latrasse D, Servet C, Zhou DX (2013) Arabidopsis histone deacetylase HDA9 regulates flowering time through repression of AGL19. Biochem Biophys Res Commun **432:** 394–398

Kölle D, Brosch G, Lechner T, Pipal A, Helliger W, Taplick J, Loidl P (1999) Different types of maize histone deacetylases are distinguished by a highly complex substrate and site specificity. Biochemistry **38:** 6769–6773

Latrasse D, Benhamed M, Henry Y, Domenichini S, Kim W, Zhou D-X, Delarue M (2008) The MYST histone acetyltransferases are essential for gametophyte development in Arabidopsis. BMC Plant Biol **8:** 121 10. 1186/1471-2229-8-121

Lawton MA, Dean SM, Dron M, Kooter JM, Kragh KM, Harrison MJ, Yu L, Tanguay L, Dixon RA, Lamb CJ (1991) Silencer region of a chalcone synthase promoter contains multiple binding sites for a factor, SBF-1, closely related to GT-1. Plant Mol Biol **16:** 235–249

Leah R, Skriver K, Knudsen S, Ruud-Hansen J, Raikhel NV, Mundy J (1994) Identification of an enhancer/silencer sequence directing the aleurone-specific expression of a barley chitinase gene. Plant J **6:** 579–589

Liu C, Li LC, Chen WQ, Chen X, Xu ZH, Bai SN (2013) HDA18 affects cell fate in *Arabidopsis* root epidermis via histone acetylation at four kinase genes. Plant Cell **25:** 257–269

Liu Z, Makaroff CA (2006) *Arabidopsis* separase AESP is essential for embryo development and the release of cohesin during meiosis. Plant Cell **18:** 1213–1225

Long JA, Ohno C, Smith ZR, Meyerowitz EM (2006) TOPLESS regulates apical embryonic fate in *Arabidopsis*. Science **312:** 1520–1523

Meinke DW, Franzmann LH, Nickle TC, Yeung EC (1994) Leafy cotyledon mutants of *Arabidopsis*. Plant Cell **6:** 1049–1064

O'Sullivan RJ, Kubicek S, Schreiber SL, Karlseder J (2010) Reduced histone biosynthesis and chromatin changes arising from a damage signal at telomeres. Nat Struct Mol Biol **17:** 1218–1225

Pandey R, Müller A, Napoli CA, Selinger DA, Pikaard CS, Richards EJ, Bender J, Mount DW, Jorgensen RA (2002) Analysis of histone acetyltransferase and histone deacetylase families of Arabidopsis thaliana suggests functional diversification of chromatin modification among multicellular eukaryotes. Nucleic Acids Res **30:** 5036–5055

Perrella G, Consiglio F, Aiese Cigliano R, Barra L, Cremona G, Sanchez-Moran E, Errico A, Bressan R, Franklin FCH, Conicella C (2010) Histone hyperacetylation affects meiotic recombination and chromosome segregation in Arabidopsis. Plant J **62:** 796–806

Ponte I, Guillén P, Debón RM, Reina M, Aragay A, Espel E, Di Fonzo N, Palau J (1994) Narrow A/T-rich zones present at the distal 5′-flanking sequences of the zein genes Zc1 and Zc2 bind a unique 30 kDa HMG-like protein. Plant Mol Biol **26:** 1893–1906

Rundlett SE, Carmen AA, Kobayashi R, Bavykin S, Turner BM, Grunstein M (1996) HDA1 and RPD3 are members of distinct yeast histone deacetylase complexes that regulate silencing and transcription. Proc Natl Acad Sci USA **93:** 14503–14508

Schmid M, Davison TS, Henz SR, Pape UJ, Demar M, Vingron M, Schölkopf B, Weigel D, Lohmann JU (2005) A gene expression map of Arabidopsis thaliana development. Nat Genet **37:** 501–506

Schwab R, Ossowski S, Warthmann N, Weigel D (2010) Directed gene silencing with artificial microRNAs. Methods Mol Biol **592:** 71–88

Sessa G, Morelli G, Ruberti I (1993) The Athb-1 and -2 HD-Zip domains homodimerize forming complexes of different DNA binding specificities. EMBO J **12:** 3507–3517

Smyth DR, Bowman JL, Meyerowitz EM (1990) Early flower development in *Arabidopsis*. Plant Cell **2:** 755–767

Soria G, Polo SE, Almouzni G (2012) Prime, repair, restore: the active role of chromatin in the DNA damage response. Mol Cell **46:** 722–734

Sprunck S, Gross-Hardt R (2011) Nuclear behavior, cell polarity, and cell specification in the female gametophyte. Sex Plant Reprod **24:** 123–136

Tanaka M, Kikuchi A, Kamada H (2008) The Arabidopsis histone deacetylases HDA6 and HDA19 contribute to the repression of embryonic properties after germination. Plant Physiol **146:** 149–161

Tian L, Fong MP, Wang JJ, Wei NE, Jiang H, Doerge RW, Chen ZJ (2005) Reversible histone acetylation and deacetylation mediate genome-wide, promoter-dependent and locus-specific changes in gene expression during plant development. Genetics **169:** 337–345

Tian L, Wang J, Fong MP, Chen M, Cao H, Gelvin SB, Chen ZJ (2003) Genetic control of developmental changes induced by disruption of Arabidopsis histone deacetylase 1 (AtHD1) expression. Genetics **165:** 399–409

Tinker-Kulberg RL, Morgan DO (1999) Pds1 and Esp1 control both anaphase and mitotic exit in normal cells and after DNA damage. Genes Dev **13:** 1936–1949

Tjaden G, Edwards JW, Coruzzi GM (1995) *Ccis* Elements and *trans*-acting factors affecting regulation of a nonphotosynthetic light-egulated gene for chloroplast glutamine synthetase. Plant Physiol **108:** 1109–1117

Varotto S, Locatelli S, Canova S, Pipal A, Motto M, Rossi V (2003) Expression profile and cellular localization of maize Rpd3-type histone deacetylases during plant development. Plant Physiol **133:** 606–617

Weigel D, Glazebrook J (2002) Arabidopsis: A Laboratory Manual. Cold Spring Harbor Laboratory Press, Cold Spring Harbor, NY

Wu K, Tian L, Malik K, Brown D, Miki B (2000) Functional analysis of HD2 histone deacetylase homologues in Arabidopsis thaliana. Plant J **22:** 19–27

Yang X, Boateng KA, Yuan L, Wu S, Baskin TI, Makaroff CA (2011) The radially swollen 4 separase mutation of Arabidopsis thaliana blocks chromosome disjunction and disrupts the radial microtubule system in meiocytes. PLoS ONE **6:** e19459

Zhou C, Labbe H, Sridha S, Wang L, Tian L, Latoszek-Green M, Yang Z, Brown D, Miki B, Wu K (2004) Expression and function of HD2-type histone deacetylases in *Arabidopsis* development. Plant J **38:** 715–724